Tetrahedron: *Asymmetry* 22 (2011) 270–276

Contents lists available at ScienceDirect

Tetrahedron: *Asymmetry*

journal homepage: www.elsevier.com/locate/tetasy

Determination of the absolute configuration of the enantiomers of dihydroquinolines, isolated by chiral chromatography, by non empirical analysis of circular dichroism spectra and X-ray analysis

Salvatore Caccamese [a,*], Giovanni Battista Barrano [a], Mateo Alajarin [b], Baltasar Bonillo [b], Ángel Vidal [b], Giuseppe Bruno [c], Giuseppe Mazzeo [d,*], Carlo Rosini [d]

[a] *Dipartimento di Scienze Chimiche, Università di Catania, Viale Andrea Doria 6, 95125 Catania, Italy*
[b] *Departamento de Quìmica Orgànica, Universidad de Murcia Campus de Espinardo, 30100 Murcia, Spain*
[c] *Dipartimento di Chimica Inorganica, Chimica Analitica e Fisica, Università di Messina, Salita Sperone 31, Vill. S. Agata, 98166 Messina, Italy*
[d] *Dipartimento di Chimica, Università della Basilicata, Via N. Sauro 85, 85100 Potenza, Italy*

ARTICLE INFO

Article history:
Received 8 December 2010
Accepted 12 January 2011
Available online 4 March 2011

Dedicated to the memory of Carlo Rosini (1948–2010), an outstanding scientist, a dear friend, and an unforgettable colleague

ABSTRACT

The enantiomers of racemic 3,4-dihydroquinolines with an acetal or thioacetal spiro ring and a quaternary stereogenic carbon have been isolated through semipreparative chiral chromatography using a polysaccharide-derived chiral stationary phase (Chiralpak AD) and *n*-hexane/ethanol as a mobile phase. The absolute configurations of the enantiomers of four compounds have been determined by a comparison of density functional theory (DFT) calculations of their electronic circular dichroism (ECD) spectra with the experimental ECD data. A detailed conformer population search to achieve a conformational average of these compounds was crucial, due to the flexibility of these molecules. The conformer distribution was evaluated by SPARTAN 02 and the structure of each of the conformers found within 4 kcal/mol energy range was optimized with DFT. The final calculated ECD spectrum obtained after Boltzmann averaging was compared with the ECD spectrum of the less well retained enantiomer and the correlation (*R*)/(−) was established for all compounds. The monocrystals of both enantiomers of one compound were obtained from the HPLC eluates. Their absolute configurations were determined by X-ray crystallographic analysis and confirmed by ECD analysis. In all cases, the second-eluted enantiomer in chiral HPLC exhibits an (*R*)-configuration.

1. Introduction

Quinoline-containing natural products have attracted the attention of synthetic and medicinal chemists for many decades. The quinoline ring system is found in many natural products of interest due to its wide range of biological activities.[1,2] Hydroquinolines constitute a key structural motif present in many biologically-active compounds, many of which have industrial and medicinal applications.

Dihydroquinolines are generally sensitive intermediates in the most common syntheses of their fully aromatized partners, although over the last few decades, there has been a growing interest in the preparation of stable dihydroquinoline derivatives.[3] Whereas 1,2-dihydroquinolines are by far the most common members of this class, the less abundant 3,4-dihydroquinolines are of particular interest because a number of adequately substituted derivatives have been shown to be potent inhibitors of the nitric oxide synthases.[4] The spiro-fusion of a third ring onto the heterocyclic nucleus of dihydroquinolines has provided potential drugs for treating lipoxygenase-mediated disorders.[5]

Some of us have recently reported[6] the facile preparation of chiral 3,4-dihydroquinolines with only one stereogenic centre, its quaternary carbon 3, and bearing spiro-fused five and six-membered saturated heterocyclic rings at carbon 4. These compounds were obtained in racemic forms due to the absence of absolute chirality sources in the synthetic sequences used for their preparation, with a 6π-electrocyclization as the final key step, whereas alternative and efficient enantioselective syntheses seem, at first sight, not easily conceivable.

Herein our aim was to assign the absolute configuration of the enantiomers of 3,4-dihydroquinolines **1**–**4** synthesized as racemic mixtures.

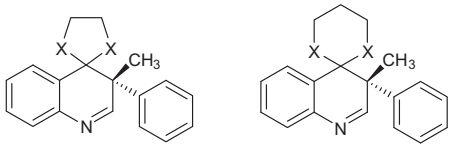

1 X = O
3 X = S
Chemical Structures
4 X = O
2 X = S

* Corresponding authors. Tel.: +39 95 7385029 (S.C.); +39 971 205478 (G.M.).
E-mail address: scaccamese@dipchi.unict.it (S. Caccamese).

0957-4166/$ - see front matter © 2011 Elsevier Ltd. All rights reserved.
doi:10.1016/j.tetasy.2011.01.010

To perform this task, we isolated the single enantiomers of **1**–**4** through semipreparative enantioselective HPLC, employed an ab initio calculation of the electronic dichroism spectra (ECD) of the enantiomers and performed a comparison of the calculated and experimental ECD spectra of the single enantiomers to assign their absolute configurations. A critical point was the calculation of the ECD spectra of stable conformer of an enantiomer, since the sign for Cotton effects can be different in different conformers. Thus, the overall calculated ECD spectrum originates from a Boltzmann average of spectra of differently populated conformers. Subsequently, the XRD structures of (+)- and (−)-**4** were solved and the absolute configuration obtained with this method confirmed the absolute configuration obtained by previous ECD calculations.

2. Results and discussion

2.1. Enantioselective chromatography

To obtain the pure enantiomers of racemic **1**–**4**, we carried out a preparative HPLC analysis using a polysaccharide-derived chiral stationary phase (CSP) under normal phase conditions (*n*-hexane/ethanol). These CSPs have a broad applicability and are widely used also for preparative purposes.[7] From several CSPs available in our laboratory, we chose Chiralpak AD because amongst the four most used polysaccharide-derived CSPs, it is the most efficient in terms of enantioseparation according to statistics from over 1000 racemic discovery compounds.[8] This observation does not leave out, however, the possibility that the performances of various CSPs can be very different with regard to the same analyte.[9] Our choice was satisfactory and the resolution was optimized by varying the amount of the alcohol (the modifier). As shown in Table 1, the separation factor α was good and it was slightly affected by the polarity of the mobile phase. Also, the resolution factor R_s remained high in all experiments.

Figure 1 shows the HPLC chromatograms of racemic **1**–**4**, using *n*-hexane/ethanol 90:10 as the mobile phase. On the basis of the analytical chromatographic results, the preparative isolation of the enantiomers of racemic **1**–**4** was carried out using experimental conditions that ensured reasonable elution times, with still good R_s and adequate loading capacity. A 1.0 cm internal diameter Chiralpak AD column was used and 10–15 replicate injections of 100–150 μL of a solution of 15 mg/mL in *n*-hexane/ethanol 80:20 of compounds **1**, **3** and **4** and 5 mg/mL of compound **2** were carried out.

Figure 2 shows the typical replicate separations of the enantiomers of (±)-**1**. Collection of the eluate corresponding to the two major chromatographic peaks, centrifugation at 5000×*g* for 10 min and rotoevaporation of the supernatants furnished about 3 mg of the single enantiomers of **1**, **3** and **4** and 1.5 mg of the single enantiomers of **2**, all as white powders. Recrystallization of the pure enantiomers of compound **4** by standing for a few days in a screw-cap vial of an ethanolic solution afforded crystals, which were used for XRD analysis. The ee values of the single enantiomers of **1**–**4** were checked by enantioselective HPLC using the conditions described in Table 1, giving values greater than 98% with an overall recovery of about 30%. The low recovery is due to the presence of sizeable amounts of impurities in the samples, as shown in Figure 2 and from a partial retention of the compounds in the column.

Table 1
Enantioselective HPLC resolution of 3,4-dihydroquinolines **1**–**4** on Chiralpak AD

Compd	A^a (%)	k'_1 [b]	t_1	t_2	α^c	R_s[d]
1	10	1.66	8.1	13.0	1.97	6.8
1	25	0.90	5.8	8.4	1.93	6.1
2	10	1.96	9.0	12.9	1.64	5.4
2	25	1.16	6.6	8.8	1.63	4.4
3	10	1.75	8.4	9.8	1.27	2.6
3	25	1.04	6.2	7.0	1.25	2.0
4	10	0.76	5.4	6.3	1.42	2.5
4	25	0.42	4.3	4.9	1.41	1.5

[a] Percentage of ethanol in *n*-hexane at a flow rate of 1 mL/min; t_0, min = 3.0.
[b] Retention factor of the first eluted enantiomer.
[c] Separation factor.
[d] Resolution factor.

2.2. Electronic circular dichroism

The ECD spectra of the enantiomers of **1**–**4**, isolated by semipreparative chiral HPLC as previously described, were measured using 4–9 × 10^{-3} solutions in ethanol. These spectra were mirror images of each other, as shown in Figure 3 for compound **1**, confirming their enantiomeric nature.

The spectra also exhibited two clear Cotton effects. Remarkably, as can be observed in the experimental ECD spectra of the second-eluted enantiomers reported in the black line in Figure 6, the ellipticity at longer wavelengths is higher for the thioacetals **2** and **3**, while the ellipticity is higher at shorter wavelengths for the corresponding acetals **1** and **4**. Thus, sulfur, due to a different electronic configuration, significantly affected the ECD spectra. At this point, due to the bisignate spectra, the presence of three different chromophores in the molecule and the difference between acetal and thioacetal spectra, it was worthwhile for us to carry out a careful and detailed analysis of the ECD spectra of the single enantiomers of **1**–**4** in order to assign their absolute configuration by the comparison of the predicted and experimental spectra. Indeed, our experience in this field, with flexible molecules, was noteworthy.[10]

2.3. Ab initio ECD calculations and the absolute configuration determination of 1–4

Nowadays the analysis of ECD spectra can be carried out using ab initio techniques, leading to safe structural determinations, such as the assignment of the molecular absolute configuration.[11–13] We decided to simulate the experimental ECD spectra of **1**–**4** by means of the Time Dependent Density Functional Theory (TDDFT) method, using the widely used hybrid functional B3LYP,[14] which, with the 6-31G* (or higher) basis set is being increasingly used by organic chemists for the determination of the absolute configuration of small and complex molecules. Representative examples for synthetic[15] and natural compounds[16] have recently appeared. Theoretical ECD spectra were obtained by means of the GAUSSIAN09 package,[17] both in the length and velocity representation, using the lowest 50 states, from excitation energies and rotational strengths, as a sum of gaussian functions centred at the wavelength of each transition, with a parameter σ (width of the band at 1/*e* height) of 0.15 eV.[18]

The ECD spectra were calculated both in the length and velocity formalisms to guarantee origin independence and to evaluate the quality of the molecular wave functions employed.[19] These calculated spectra were almost coincident, indicating a good level of calculation. For this reason in all figures, only the velocity-form predicted spectra are reported. In practice, to simulate the experimental ECD spectra of compounds **1**–**4**, we arbitrarily assumed an (*R*)-absolute configuration for the stereogenic centre.

Due to the flexibility of the molecules, conformational analysis at a molecular mechanics level led to four most populated conformers for **1**, seven for **2**, six for **3** and seven for **4**. The structures of the conformers were then fully optimized at DFT/B3LYP/6-31G* level. After free energy calculation we employed a Boltzmann distribution to calculate the conformer populations. In Figure 4, we show the structures, Boltzmann distributions and relative

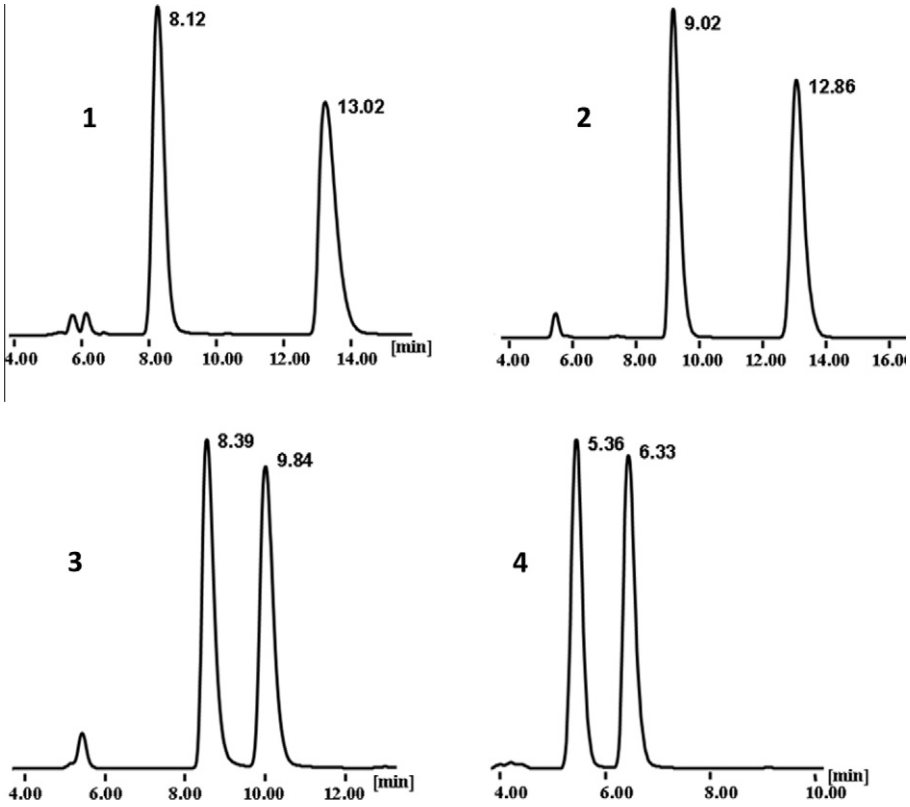

Figure 1. Typical separation of the enantiomers of compounds **1**–**4**. Conditions as line 1 (**1**), line 3 (**2**), line 5 (**3**), line 7 (**4**) in Table 1.

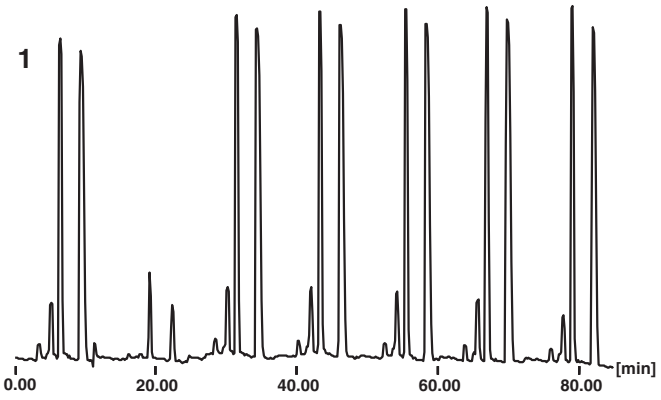

Figure 2. Typical replicate separation of the enantiomers of compound **1** with a semipreparative Chiralpak AD column.

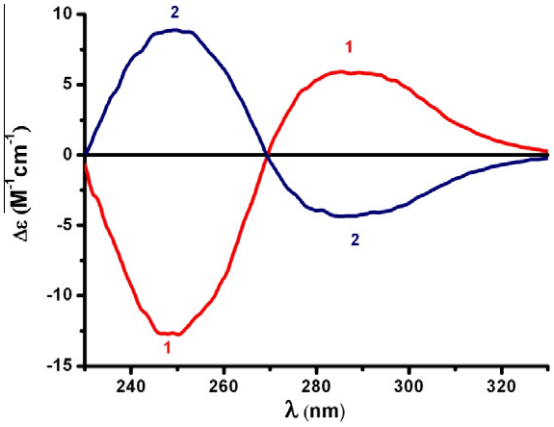

Figure 3. CD spectra of isolated enantiomers of compd. **1** . First (1) and second (2) HPLC peaks, in ethanol (4×10^{-3} M) and 1mm cell.

conformer energies (in kcal/mol) of the (*R*)-enantiomers of compounds **1**–**4**.

As shown, these conformers differ from each other by the sense of the twist of the five and six membered acetal and thioacetal rings and by the phenyl position (equatorial/axial) at the stereogenic carbon.

As expected, the equatorial phenyl conformer is the most stable. In order to save computational effort and time, ECD calculations were performed only on about 98% of the overall conformer population. The direction of the electric transition dipole moments is quite different in conformers where the phenyl ring at the stereogenic carbon is equatorial with respect to the conformers where this phenyl is axial. As a consequence, the ECD spectra of the conformers strongly differ and the sign of the Cotton effect changes in some cases, as shown for example for conformers **4a**–**4d** in Figure 5, for the same assumed (*R*)-configuration. With a TDDFT/B3LYP/6-31G* level of calculation we achieved a good agreement between the experimental and calculated ECD saving computational effort and avoiding the use of larger basis sets. In Figure 6, the comparisons between experimental ECD spectra (experimental ECD, black line) together with the overall calculated ones (theoretical ECD, grey line) of compounds **1**–**4** are displayed. The experimental ECD spectra regard the (−)-enantiomer, which is the second eluted one.

All calculations correctly reproduced the number and sign of the observed Cotton effects at about 290 nm and 260 nm, even if a clear red shift[20] of the theoretical bands with respect to the experimental spectra can be noticed. For **2** and **3**, the theoretical ECD spectra (Fig. 6) were reduced four times. The good agreement

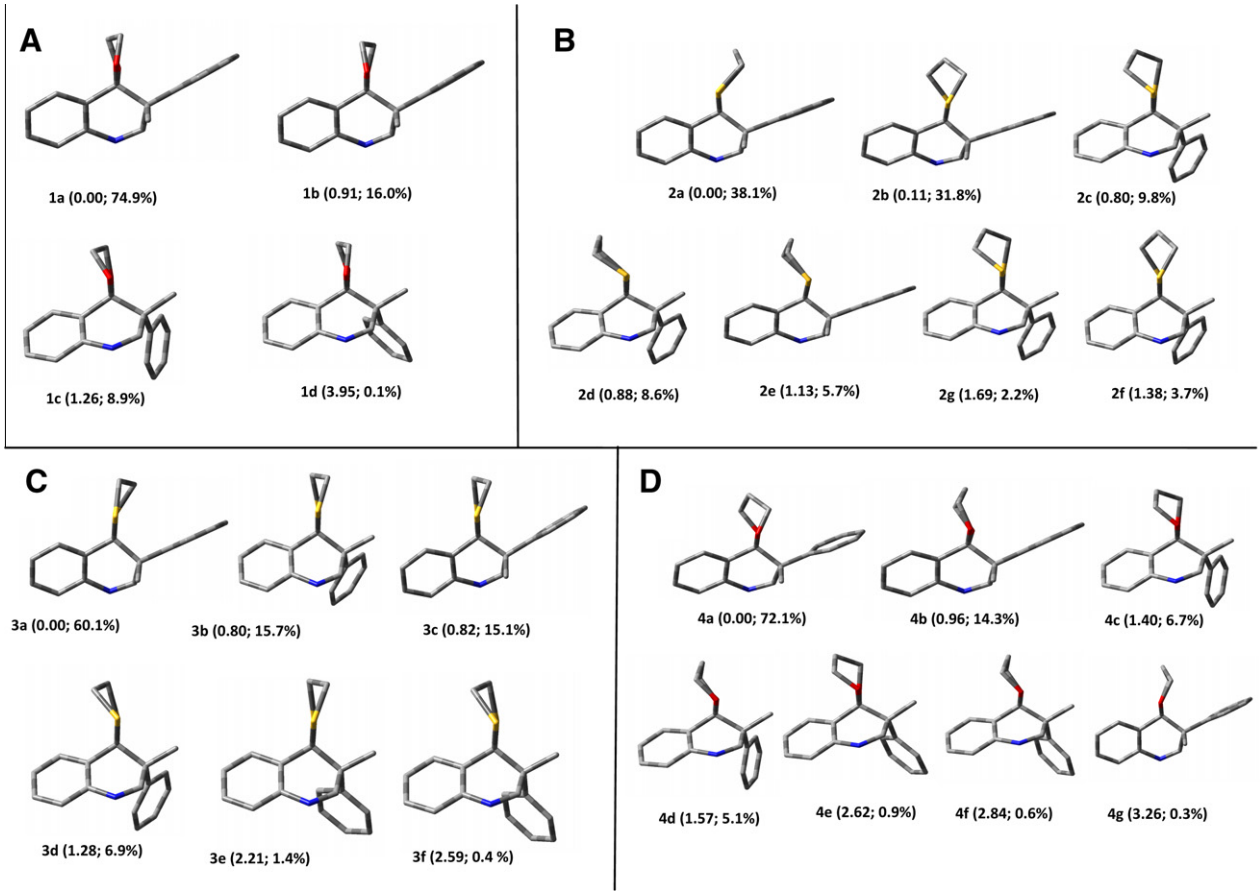

Figure 4. Structures of the most stable conformers of (*R*)-enantiomer of compounds **1**–**4** optimized at the B3LYP/ 6-31G* level and their relative energies (in kcal mol^{-1}) and populations (in brackets, respectively). A: (*R*)-**1** (1a-d); B: (*R*)-**2** (2a-g); C: (*R*)-**3** (3a-f); D: (*R*)-**4** (4a-g).

between calculated and experimental spectra strongly supports the (*R*)/(−) absolute configuration assignment.

2.4. Single crystal X-ray analysis

The assignment of the absolute configuration of the enantiomers of **4** was then confirmed by X-ray analysis of single crystals obtained in small amounts by enantioselective HPLC. Both (*S*)-**4** and (*R*)-**4** crystallize in the $P2_12_12_1$ space group with a molecule in the asymmetric unit. The corresponding Flack parameter for (*S*)-**4** was found to be 0.0(3), and for (*R*)-**4** was determined to be −0.2(4). The details of the crystal structure determination and refinements for compounds (*S*)-**4** and (*R*)-**4** are given in Table 2. An ORTEP view of both enantiomers is shown in Figure 7.

These values are all comparable with the corresponding structural parameters reported for similar compounds reported in the Crystallographic Data Centre.[21] Puckering parameters indicate a distorted envelope conformation of the dihydropyridine hexatomic ring, while the cyclic acetal ring shows an ideal chair conformation. Molecular packing is mainly determined by Van der Waals interactions and few weak hydrogen bonds involving both O1 and O2 acetal oxygen atoms.

Furthermore, a weak intermolecular H–π hydrogen bond involves a methyl hydrogen atom and the phenyl group bonded to the stereogenic carbon atom at C17 [H···Ph-Centroid 2.816(3) Å].

Crystallographic data (excluding structure factors) for (*S*)-**4** and (*R*)-**4** have been deposited with the Cambridge Crystallographic Data Centre as Supplementary Publication Numbers CCDC 776100 [for (*S*)-**4**] and CCDC 776101 [for (*R*)-**4**]. Copies of the data can be obtained, free of charge, on an application to CCDC, 12 Union Road, Cambridge CB2 1EZ, UK [fax +44(0)1223 336033 or e-mail: deposit@ccdc.cam.ac.uk].

3. Conclusions

We have presented the isolation of the enantiomers of four 3,4-dihydroquinolines through semipreparative chiral HPLC. The absolute configurations of the enantiomers were determined by comparison of the measured and calculated ECD spectra. The flexibility of these molecules made a detailed conformational distribution search necessary, including calculation of the ECD spectra of several conformers and Boltzmann-weighted superimposition of the ECD of the single conformers. We have shown that a good agreement between experimental and calculated ECD can be achieved using TDDFT calculations with a simple basis set at 6-31G* level and correct input geometry of several conformers. The absolute configurations were then confirmed by X-ray crystal structure determination of both enantiomers of one compound.

4. Experimental section

4.1. Starting materials

Racemic compounds **1** and **3** were synthesized as previously described.[6] Racemic compounds **2** and **4** were prepared following the same synthetic procedure but using 1,3-propanedithiol and 1,3-propanediol, respectively, as reagents in the first step of the synthetic sequence, the acetalization of 2-azidobenzaldehyde.

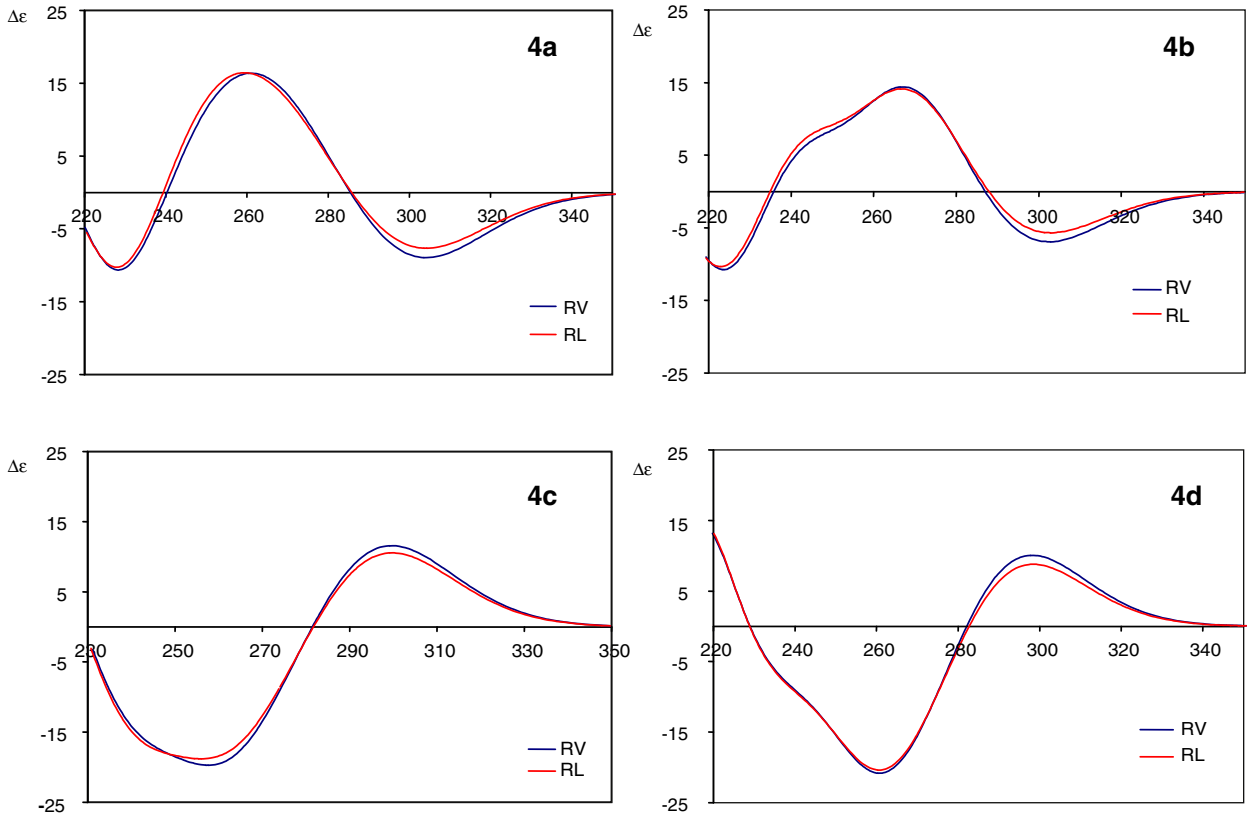

Figure 5. Simulated ECD spectra of conformers (98.2% of overall populations) of compound **4**, as obtained at the TDDFT/B3LYP/6-31G* level, velocity (RV) and length (RL) formalism, using the lowest 50 states on the DFT/B3LYP/6-31G* geometry.

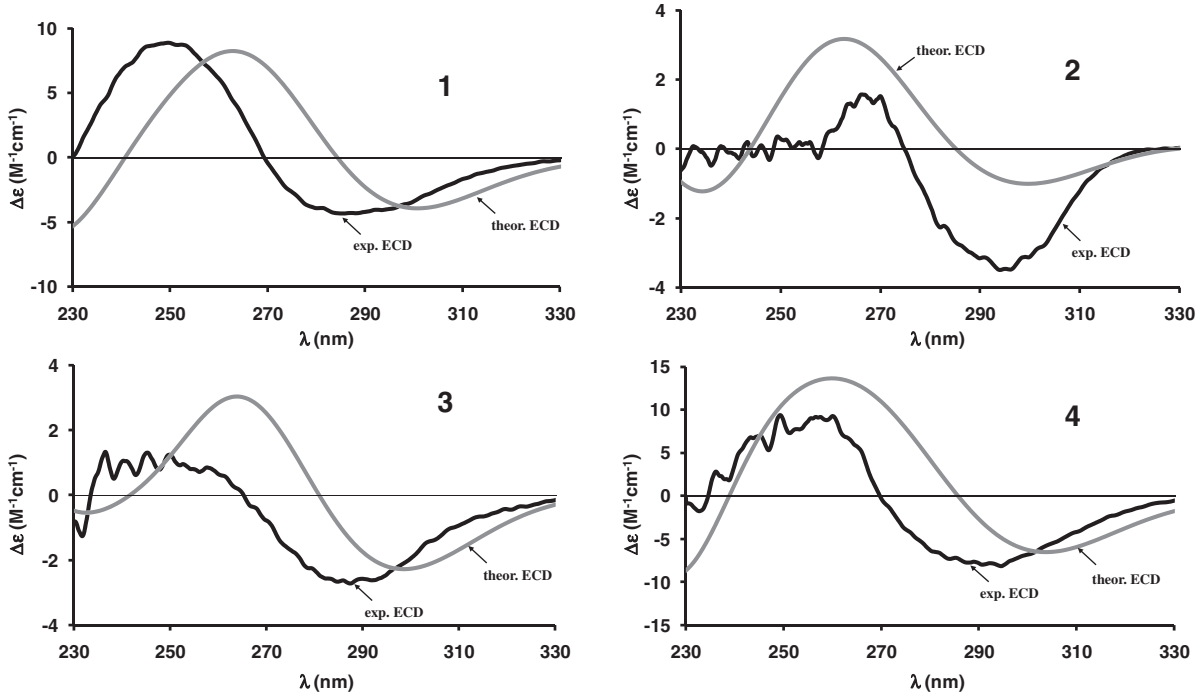

Figure 6. Averaged calculated CD spectra of (*R*)-configuration of compounds **1**–**4** (grey line). Experimental CD spectra of the second eluted enantiomer in chiral HPLC of compounds **1**–**4** (black line).

Table 2
Crystal data and structure refinement for (*S*)-**4** and (*R*)-**4**

Enantiomer	*S*	*R*
Empirical formula	$C_{19}H_{19}NO_2$	
Formula weight	293.35	
Crystal system, space group	Orthorhombic, $P2_12_12_1$ (*N*. 19)	
Unit cell dimensions	a = 8.57590(10) Å	a = 8.5759(2) Å
	b = 11.9996(2) Å	b = 11.9992(3) Å
	c = 14.6026(2) Å	c = 14.5998(3) Å
Volume	1502.72(4) Å^3	1502.38(6) Å^3
Z	4	
Density (calculated)	1.297 Mg/m^3	
Absorption coefficient	0.084 mm^{-1} (λ = 0.71073 Å)	
F(0 0 0)	624	
Crystal size	0.68 × 0.52 × 0.43 mm^3	0.41 × 0.30 × 0.23 mm^3
Theta range for data collection	2.75–25.00°	
Index ranges	$10 \le h \le 10$, $-14 \le k \le 14$, $-17 \le l \le 17$	
Reflections collected	43447	79943
Independent reflections	2645 [R(int) = 0.0201]	2641 [R(int) = 0.0204]
Completeness to θ = 25.00°	99.8%	99.7%
Refinement method	Full-matrix least-squares on F^2	
Data/restraints/parameters	2645/0/200	2641/0/200
Goodness-of-fit on F^2	0.800	1.014
Final R indices [$I > 2\sigma(I)$]	R_1 = 0.0259,	R_1 = 0.0253,
	wR_2 = 0.0747	wR_2 = 0.0704
R indices (all data)	R_1 = 0.0262,	R_1 = 0.0255,
	wR_2 = 0.0754	wR_2 = 0.0709
Flack parameter	0.0(3)	−0.2(4)
Largest diff. peak and hole	0.135/−0.114 e Å^{-3}	0.140/−0.101 e Å^{-3}

4.2. 3′-Methyl-3′-phenylspiro[1,3-dithiane-2,4′(3′*H*)-quinoline] 2

Obtained by heating a solution of the corresponding ketenimine in anhydrous toluene for 24 h (60% yield). Colourless prisms (diethyl ether). Mp: 141–143 °C. IR (Nujol) ν: 1633 (vs), 1591 (m), 1311 (s), 1274 (m), 1213 (m), 1108 (w), 972 (w), 879 (w), 756 (s), 721 (s), 675 (m) cm^{-1}. ^{1}H NMR (300 MHz, $CDCl_3$, 25 °C) δ: 1.64 (s, 3 H), 1.66–1.84 (m, 2 H), 2.15–2.32 (m, 2 H), 2.48–2.57 (m, 2 H), 7.25–7.39 (m, 5 H), 7.46 (dd, 1 H, J = 7.5, 1.5 Hz), 7.58–7.62 (m, 2 H), 7.95 (dd, 1 H, J = 7.5, 1.5 Hz), 8.16 (s, 1H). ^{13}C NMR (75 MHz, $CDCl_3$, 25 °C) δ: 18.7, 23.1, 26.9, 27.0, 51.2 (s), 60.6 (s), 126.3, 127.6, 127.8, 128.1, 128.7, 130.0, 132.2 (s), 138.7 (s), 140.9 (s), 168.9. MS (70 eV, EI): *m/z* (%): 325 (M$^+$, 6), 251 (46), 250 (100), 219 (58), 218 (41), 217 (23), 204 (22), 103 (29), 77 (21). Elemental Anal. Calcd for $C_{19}H_{19}NS_2$ (325.50): C, 70.11; H, 5.88; N, 4.30. Found: C, 69.90; H, 5.80; N, 4.14.

4.3. 3′-Methyl-3′-phenylspiro[1,3-dioxane-2,4′(3′*H*)-quinoline] 4

Obtained by heating a solution of the corresponding ketenimine in anhydrous *o*-xylene for 24 h (81% yield). Colourless prisms (diethyl ether). Mp: 154–155 °C. IR (Nujol) ν: 1618 (m), 1598 (w), 1496 (w), 1215 (s), 1178 (w), 1141 (m), 1118 (s), 1093 (vs), 1054 (w), 1033 (m), 1024 (m), 973 (m), 962 (m), 929 (w), 904 (w), 877 (w), 846 (w), 773 (vs), 761 (m) cm^{-1}. ^{1}H NMR (300 MHz, $CDCl_3$, 25 °C) δ: 1.47 (s, 3 H), 1.55–1.66 (m, 1 H), 1.72–1.84 (m, 1 H), 3.17–3.25 (m, 1 H), 3.53–3.73 (m, 3 H), 7.24–7.36 (m, 4 H), 7.37–7.40 (m, 1 H), 7.42–7.51 (m, 3 H), 7.63 (dd, 1 H, J = 7.4, 1.0 Hz), 8.06 (s, 1 H). ^{13}C NMR (75 MHz, $CDCl_3$, 25 °C) δ: 16.7, 24.7, 51.4 (s), 58.2, 59.7, 98.7 (s), 125.3, 127.1, 127.2, 127.6, 128.8 (s), 129.4, 129.5, 138.9 (s), 143.4 (s), 171.3. MS (70 eV, EI): *m/z* (%): 293 (M$^+$, 50), 251 (69), 250 (89), 234 (100), 220 (59), 206 (90), 130 (63), 103 (83), 77 (74). Elemental Anal. Calcd for $C_{19}H_{19}NO_2$ (293.37): C, 77.79; H, 6.53; N, 4.77. Found: C, 77.98; H, 6.67; N, 4.65.

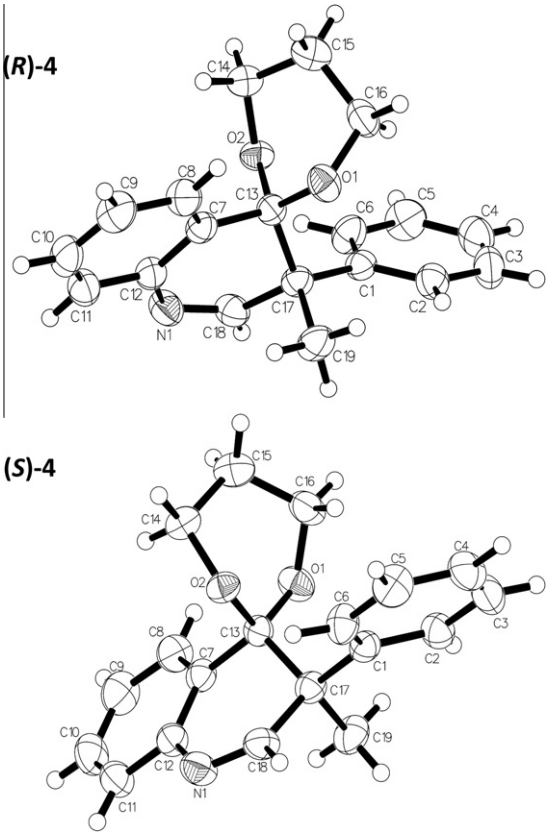

Figure 7. X-ray crystal structure of both enantiomers of compound 4 [(*R*) on the top and (*S*) on the bottom] in their asymmetric unit showing the numbering scheme. Thermal ellipsoids are drawn at the 50% of probability level while hydrogen size is arbitrary.

4.4. Enantioselective HPLC

The analytical resolution of **1–4** was performed on a polysaccharide-derived column (250 mm × 4.6 mm i.d.) Chiralpak AD (amylose tris[3,5-dimethylphenylcarbamate] coated on 5 μm silica gel. For the semipreparative isolation of the enantiomers, a Chiralpak AD column size 250 mm × 10 mm i.d. was used. Both columns were purchased from Chiral Technologies (Illkirch, France). A column in-line filter with 0.5 μm stainless steel frit of 3 mm diameter was used to protect the HPLC column. Column void volume (t_0) was measured by injection of tri-*tert*-butylbenzene as a nonretained sample.[22] The HPLC parameters (k, α, and R_s) were those typically employed.[23] The HPLC system consisted of a PU 980 pump, a LG-1580-02 low pressure mixer, and a DG-1580-54 in line degasser with a Rheodyne injection valve equipped with 20 or 200 μL sample loops, a Uvidec 100-III UV spectrophotometric detector operating at 235 nm (all from Jasco). Chromatograms were acquired and processed using a computer-based Jasco Borwin 2 software.

4.5. Chiroptical measurements

The ECD spectra were measured in ethanol on a Jasco 810 spectropolarimeter using a 1 mm cell and scanning ten times from 350 to 230 nm at 50 nm/min.

4.6. Computational details

All calculations were carried out on a simple PC endowed with a Intel(R) Xeon Quadcore E5420 at 2.50 GHz. The preliminary conformational distribution search has been performed by the SPARTAN02 package[24] using the MMFF94s molecular mechanics force field.

The 'Systematic' and 'Montecarlo' options were used and search of all possible conformers has been performed, considering the degrees of freedom of system and retaining only the structures with an energy of not more than 4 kcal/mol above the most stable conformer. The real minimum energy conformers found by molecular mechanics have been further fully optimized at the DFT/B3LYP/6-31G* level as implemented in the GAUSSIAN09 package.[17] All conformers are real minima, no imaginary vibrational frequencies have been found and the free energy values have been calculated and used to get the Boltzmann population of conformers at 298.15 K. The ECD calculations were carried out by means of time-dependent DFT methods using the hybrid B3LYP functional and the 6-31G* as available within GAUSSIAN09. All calculations were performed in gas phase avoiding more computational effort due to application of solvation models.

4.7. X-ray data collection and structure refinement

As discussed in Section 2.1, enantioselective HPLC afforded pure enantiomers. Colourless single crystals of both enantiomers were selected for X-ray structural analysis from the crystals obtained from enantioselective HPLC. Data were collected at room temperature with a Bruker APEX II CCD area-detector diffractometer and graphite-monochromatized Mo Kα radiation (λ = 0.71073 Å). Data collection, cell refinement, data reduction and absorption correction by a multi-scan method were performed by the programmes of the Bruker software. The structure was solved by direct methods using XS97.[25] The non-hydrogen atoms were refined anisotropically by the full-matrix least-squares method on F2 using SHELXL-97.[26] All H atoms were introduced in calculated positions and constrained to ride on their parent atoms.

Acknowledgements

G.M. and C.R. are grateful to the MIUR, Rome for financial support (PRIN 2008 'Determination of the molecular absolute configuration by means of chiroptical spectroscopies: development of new efficient methods and their application to bioactive molecules'). M.A., A.V. and B.B. thank the financial support of MICINN (Project CTQ 2008-05827/BQU) and Fundacion Seneca-CARM (Project 08661/PI/08). S.C. thanks the University of Catania (Progetti di Ricerca di Ateneo) for financial support.

References

1. Jones, G. In *The Chemistry of Heterocyclic Compounds: Quinolines*; Wiley: Chichester, 1977; Vol. 32, (pt 1), 1982 (pt. 2), 1990 (pt. 3).
2. Michael, P. *Nat. Prod. Rep.* **2001**, *17*, 603–620. and previous reviews in this series.
3. See, e.g.: (a) Evans, P. A.; Robinson, J. E.; Moffett, K. K. *Org. Lett.* **2001**, *3*, 3269–3271; (b) Parker, K. A.; Mindt, T. L. *Org. Lett.* **2002**, *4*, 4265–4268; (c) Hartline, C. B.; Harden, E. A.; Williams-Aziz, S. L.; Kushner, N. L.; Brideau, R. J.; Kern, E. R. *Antiviral Res.* **2005**, *65*, 97–105; (d) Ranu, B. C.; Hajra, A.; Dey, S. S.; Jana, U. *Tetrahedron* **2003**, *59*, 813–819.
4. (a) Jaroch, S.; Hölscher, P.; Rehwinkel, H.; Sülzle, D.; Burton, G.; Hillmann, M.; McDonald, F. M. *Bioorg. Med. Chem. Lett.* **2002**, *12*, 2561–2564; (b) Jaroch, S.; Hölscher, P.; Rehwinkel, H.; Sülzle, D.; Burton, G.; Hillmann, M.; McDonald, F. M. *Bioorg. Med. Chem. Lett.* **2003**, *13*, 1981–1984; (c) Jaroch, S.; Rehwinkel, H.; Hölscher, P.; Sülzle, D.; Hillmann, M.; Burton, G. A.; McDonald, F. M. U.S. Patent 6,391,887, 2002; *Chem. Abstr.* **1999**, *131*, 157716.
5. Chu, D. T. W.; James, D. R.; Wang, B. PCT Patent WO 2006/093548, 2006; *Chem. Abstr.* **2006**, *145*, 285195.
6. Alajarin, M.; Bonillo, B.; Ortin, M.-M.; Sanchez-Andrada, P.; Vidal, A. *Org. Lett.* **2006**, *8*, 5645–5648.
7. (a) Okamoto, Y.; Ikai, T. *Chem. Soc. Rev.* **2008**, *37*, 2593–2608; (b) Okamoto, Y.; Yashima, E. *Angew. Chem., Int. Ed.* **1998**, *37*, 1020–1043.
8. Francotte, E. Presentation at Chiral Europe June 2004, Mainz, Germany, 2004.
9. Caccamese, S.; Chillemi, R.; Perna, F. M.; Florio, S. *J. Chromatogr., A* **2009**, *1216*, 3048–3053.
10. (a) Mazzeo, G.; Giorgio, E.; Rosini, C.; Fabris, F.; Fregonese, E.; Toniolo, U.; De Lucchi, O. *Chirality* **2009**, *21*, E86–E97; (b) Tartaglia, S.; Padula, D.; Scafato, P.; Chiummiento, L.; Rosini, C. *J. Org. Chem.* **2008**, *73*, 4865–4873.
11. Koslowski, A.; Sreerama, N.; Woody, R. W. In *Circular Dichroism: Principles and Applications*; Nakanishi, K., Berova, N., Woody, R. W., Eds.; Wiley-VCH: New York, 2000; pp 55–87.
12. For a general discussion of the ab initio calculation of chiroptical properties: (a) Polavarapu, P. L. *Chirality* **2002**, *14*, 768–781; (b) Pecul, M.; Ruud, K. *Adv. Quantum. Chem.* **2005**, *50*, 185–227; (c) Crawford, T. D. *Theor. Chem. Acc.* **2006**, *115*, 227–245; (d) Stephens, P. J. In *Computational Medicinal Chemistry for Drug Discovery*; Bultinck, P., De Winter, H., Langenaecker, W., Tollenaere, J., Eds.; Dekker: New York, 2004; pp 699–725. Chapter 26.
13. For recent reviews and representative applications, see: (a) Bringmann, G.; Bruhn, T.; Maksimenka, K.; Hemberger, Y. *Eur. J. Org. Chem.* **2009**, 2717–2727; (b) Autschbach, J. *Chirality* **2009**, *21*, S116–152.
14. (a) Becke, A. D. *J. Chem. Phys.* **1993**, *985*, 648–5652; (b) Lee, C.; Yang, W.; Parr, R. G. *Phys. Rev.* **1988**, *B37*, 785–789; (c) Stephens, P. J.; Devlin, F. J.; Chabalowski, C. F.; Frisch, M. J. *J. Phys. Chem.* **1994**, *98*, 11623–11627.
15. (a) Worch, C.; Atodiresei, I.; Raabe, G.; Bolm, C. *Chem. Eur. J.* **2010**, *16*, 677–683; (b) Talotta, C.; Gaeta, C.; Troisi, F.; Monaco, G.; Zanasi, R.; Mazzeo, G.; Rosini, C.; Neri, P. *Org. Lett.* **2010**, *13*, 2912–2915; (c) Frelek, J.; Fryszkowska, A.; Kwit, M.; Ostaszewski, R. *Tetrahedron: Asymmetry* **2006**, *13*, 2469–2478; (d) Marié, J.-C.; Xiong, Y.; Min, G. K.; Yeager, A. R.; Berova, N.; Schaus, S. E.; Porco, J. A. *J. Org. Chem.* **2010**, *75*, 4584–4590.
16. (a) Bringmann, G.; Gulder, T. A. M.; Reichert, M.; Gulder, T. *Chirality* **2008**, *20*, 628–642; (b) Bringmann, G.; Feneis, D.; God, R.; Maksimenka, K.; Mühlbacher, J.; Messer, K.; Münchbach, M.; Gulden, K. P.; Peters, E.-M.; Peters, K. *Tetrahedron* **2004**, *60*, 8143–8151; (c) Bicker, W.; Kacprzak, K.; Kwit, M.; Lämmerhofer, M.; Gawronski, J.; Lindner, W. *Tetrahedron: Asymmetry* **2009**, *20*, 1027–1035; (d) Stephens, P. J.; McCann, D. M.; Devlin, F. J.; Smith, A. B. *J. Nat. Prod.* **2006**, *69*, 1055–1064.
17. Frisch, M. J.; Trucks, G. W.; Schlegel, H. B.; Scuseria, G. E.; Robb, M. A.; Cheeseman, J. R.; Scalmani, G.; Barone, V.; Mennucci, B.; Petersson, G. A.; Nakatsuji, H.; Caricato, M.; Li, X.; Hratchian, H. P.; Izmaylov, A. F.; Bloino, J.; Zheng, G.; Sonnenberg, J. L.; Hada, M.; Ehara, M.; Toyota, K.; Fukuda, R.; Hasegawa, J.; Ishida, M.; Nakajima, T.; Honda, Y.; Kitao, O.; Nakai, H.; Vreven, T.; Montgomery, J. A., Jr.; Peralta, J. E.; Ogliaro, F.; Bearpark, M.; Heyd, J. J.; Brothers, E.; Kudin, K. N.; Staroverov, V. N.; Kobayashi, R.; Normand, J.; Raghavachari, K.; Rendell, A.; Burant, J. C.; Iyengar, S. S.; Tomasi, J.; Cossi, M.; Rega, N.; Millam, J. M.; Klene, M.; Knox, J. E.; Cross, J. B.; Bakken, V.; Adamo, C.; Jaramillo, J.; Gomperts, R.; Stratmann, R. E.; Yazyev, O.; Austin, A. J.; Cammi, R.; Pomelli, C.; Ochterski, J. W.; Martin, R. L.; Morokuma, K.; Zakrzewski, V. G.; Voth, G. A.; Salvador, P.; Dannenberg, J. J.; Dapprich, S.; Daniels, A. D.; Farkas, O.; Foresman, J. B.; Ortiz, J. V.; Cioslowski, J.; Fox, D. J. *GAUSSIAN 09, Revision A.02*; Gaussian, Inc.: Wallingford, CT, 2009.
18. Rosini, C.; Giorgio, E.; Tanaka, K.; Verotta, L.; Nakanishi, K.; Berova, N. *Chirality* **2007**, *19*, 434–445.
19. Moscowitz, A. In *Modern Quantum Chemistry*; Sinanoglu, O., Ed.; Academic Press: London, 1965; p 31. Part III.
20. Autschbach, J.; Jensen, L.; Schatz, G. C.; Electra Tse, Y. C.; Krykunov, M. *J. Phys. Chem. A* **2006**, *110*, 2461–2473.
21. Allen, F. H.; Bird, C. M.; Rowland, R. S.; Raithby, P. R. *Acta Crystallogr., Sect. B* **1997**, *53*, 696–701.
22. Koller, H.; Rimböck, K.-E.; Mannschreck, A. *J. Chromatogr.* **1983**, *282*, 89–94.
23. Allenmark, S. *Chromatographic Enantioseparation: Methods and Applications*, 2nd ed.; Ellis Horwood: Chichester, 1991. p 82.
24. *SPARTAN '02*; Wavefunction Inc.: Irvine, CA. http://www.wavefunction.com.
25. Bruker AXS Inc., Madison, Wisconsin, USA, ©2005, COSMO (Version 1.60), SAINT (Version 7.06A), SADABS (Version 2.10), SHELXS (Version 97).
26. Sheldrick, G. M. *SHELXL97, Program for Crystal Structure Refinement*; University of Göttingen, Germany, 1997.